Analysis of a Self-oscillating Bidirectional DC-DC Converter in Battery Energy Storage Applications

J. A. Barrado, *Member, IEEE*, A. El Aroudi, *Member, IEEE*, H. Valderrama-Blavi, *Member, IEEE*, J. Calvente, *Member, IEEE* and L. Martínez-Salamero, *Member, IEEE*

***Abstract*—This paper combines three different methods for the analysis of a self-oscillating bidirectional DC-DC converter under hysteresis control. First, the describing function method is used to predict the steady state limit cycle, its oscillation amplitude and frequency. Second, Tsypkin method is applied to provide more precise information on the dynamical behavior of the system. To complete the study, a sliding mode approach is used to give more insight into the system response in terms of its parameters. A comparative study among the results obtained from the different approaches in the frequency and time domain is given. Finally, an experimental prototype validates the theoretical and the numerical predictions.**

***Index Terms*—Self-oscillating converters, bidirectional DC-DC converter, describing function, Tsypkin method, sliding mode, battery energy storage system, hysteretic control.**

I. Introduction

BIDIRECTIONAL power converters are two-quadrant output systems often employed in battery charge/discharge regulators, DC uninterruptible power supplies (UPS) and DC motor controllers with regenerative braking. Their application field includes space and telecommunication systems, electric vehicles and renewable energies [1]. The UPS operation principle is based on the fact that when the DC line at the input port is active, the power converter acts as a battery charge regulator; if the line fails, the power flow reverses and the control algorithm automatically changes to provide load regulation. The requirements of a bidirectional converter in these applications are a high efficiency and a good dynamic response in both operation modes, i.e., energy transfer from input port (V_{dc}) to output port (V_{bat}) and vice-versa. The state of the art shows a great variety of topologies employed in bidirectional operation ranging from those using a simple inductive switched branch [2] to more complex structures based on a buck-boost converter [3], Ćuk converter [4], SEPIC-Luo converter [5] interleaved converters [6] and multilevel converters [7]. In some cases, galvanic isolation is provided between input and output ports when their respective DC levels are significantly different [8]-[9].

This paper presents a comprehensive study of a hysteretic controlled bidirectional DC-DC converter for a battery energy storage system (BESS) as considered in [10]. The DC-DC converter consists of a half-bridge IGBT module with a LCL filter (Fig.1). This topology is very simple and easy to operate in bidirectional mode. The chosen filter allows higher attenuation of the high frequency harmonic content in the battery current than the usual L-filter. Thus, in the low frequency region, as the sum of L_1 and L_2 is smaller than the L-filter inductance, the voltage drop across the LCL filter is lower than the L-filter case. As a result, the DC losses are lower. The LCL filter is designed primarily from L_1 ripple current, DC voltage levels and selected switching frequency; and then taking into account the components ratio and frequency response of battery filter [11].

Our proposal for regulating the converter of Fig. 1 is a hysteretic control because it is simple and can provide a fast dynamic response with a wide regulation range and additionally it will make the system to oscillate without an external oscillator. This kind of switching converters are traditionally named as *self-oscillating* converters [12]. Although the hysteretic control in power electronics is well-known since the early years of power supplies research, the resulting variable switching frequency and the required non-linear analysis for its design have relegated its use to specific applications in power distribution systems in satellites. However, the hysteresis control has recently undergone an important revival in the implementation of voltage regulation modules (VRMs), microgrids, distributed power generation systems, and other applications [13], [17].

In Fig. 1, transistors T_1 and T_2 are activated out of phase by means of signal u, so that when one transistor is in the ON state the other one is in the OFF state and vice-versa. Note that in the unidirectional direct mode, D_2 opens when the current through it tries to reverse after reaching zero in the OFF state. To facilitate this reversal, transistor T_2 is connected in parallel to carry the current. A dual reasoning leads to the inclusion of a diode in parallel with the transistor T_1. The control strategy is given by a hysteretic control law with the following output values

$$u(t) = \begin{cases} 0 & \text{if } \sigma(t) > +h, \text{ or } |\sigma(t)| < h \text{ and } \sigma(t^-) = +h \\ 1 & \text{if } \sigma(t) < -h \text{ or } |\sigma(t)| < h \text{ and } \sigma(t^-) = -h \end{cases} \quad (1)$$

where σ is the input to the hysteresis controller and t^- is the last instant when the control signal hit the switching boundaries defined by $\pm h$.

However, in spite of the simplicity of both converter topology and control of the system depicted in Fig. 1, a rigorous analysis of its dynamics showing the main guidelines for an optimum design is not a simple task due to the nonlinear

The authors are with the Departament d'Enginyeria Electrònica, Elèctrica i Automàtica, Escola Tècnica Superior d'Enginyeria, Universitat Rovira i Virgili, 43007, Tarragona, Spain (e-mail:joseantonio.barrado@urv.cat).

This work was partially supported by the Spanish Ministerio de Educación e Innovación under grants DPI2010-16481, DPI2009-14713-C03-02, DPI2010-16084 and CSD2009-00046.

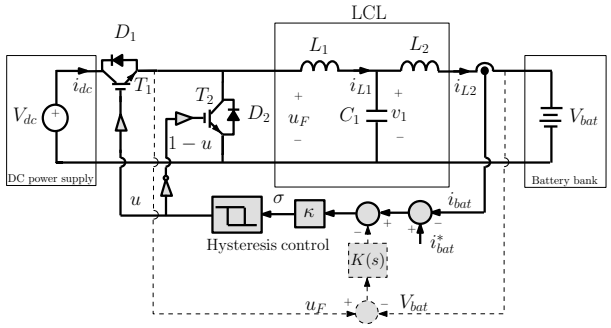

Fig. 1. Hysteresis control-based of a bidirectional buck converter with output inductor.

behavior of the power stage and the regulation loop. In the work here reported, we undertake the design-oriented analysis of the bidirectional structure of Fig. 1 by means of three different approaches: 1) Describing Function (DF) [18]. 2) Tsypkin technique [19] and 3) sliding mode (SM) control based on the equivalent control method [20]. A comparison among the different approaches is also carried out. The remaining of this paper is organized as follows. In section II the system description and modeling is addressed. Section III will deal with the DF-based analysis of the system dynamic behavior. The Tsypkin method is applied in Section IV to the hysteretic controlled system including a compensating network. Section V will present more analytical details on the system dynamic behavior by using a SM approach. Section VI shows some numerical simulations from a switched model of the system and discuss the problem of coexistence of multiple limit cycles detected in the system. Experimental validation of the results obtained by numerical simulations and theoretical predictions is illustrated in Section VII. Finally some concluding remarks are drawn in the last section.

II. System Modeling

The LCL filter in Fig. 1 is modeled as a transfer function $L(s)$ that relates the output current of the stage to the applied square wave voltage u_F. Note that the current i_{bat} through the battery is the same as i_2 through inductor L_2. The expression of the transfer function $L(s)$ is given by

$$\frac{I_{L2}(s)}{U_F(s)} := L(s) = \frac{1}{a_3 s^3 + a_2 s^2 + a_1 s + a_0} \tag{2}$$

where

$$a_3 = C_1 L_1 L_2, \qquad a_2 = C_1(L_1 r_2 + L_2 r_1)$$
$$a_1 = C_1 r_1 r_2 + L_1 + L_2, \qquad a_0 = r_1 + r_2$$

r_1 represents the parasitic resistance in the inductor L_1 and r_2 is the sum of the parasitic resistance of L_2 and the internal resistance in the battery bank.

The fact of using a hysteresis control will lead the converter to a self-oscillating mode, where the switching frequency f_0 is fixed by the value of the hysteresis width h and the parameters of the linear part of the system. Hence, the voltage at the LCL filter input switches between two values ($u_F = V_{dc}$ and $u_F = 0$) with a certain duty cycle δ and switching frequency.

III. Describing Function-Based Analysis

A. Describing function technique

The DF is a quasi-linear approximation of a non-linear element by a linear system that depends on the amplitude of the input waveform. This method can be explained by means of the decomposition of the system in a linear and a nonlinear part [18]. The frequency response $L(j\omega)$ of the linear part must have a low pass filter behavior and the nonlinear part must be symmetric and time invariant.

In this technique, the reference input is set to zero and the amplified error signal $\sigma(t)$ is approximated by its first harmonic ($\sigma(t) = S_1 \sin(\omega t)$), where S_1 is the amplitude and ω is the oscillation frequency [1]. Due to the nonlinear element, the output is distorted so that the signal u_F is periodic in steady state but non sinusoidal. The first harmonic of $u_F(t)$ is $u_{F1}(t) = U_1 \sin(\omega t + \phi_U(\omega))$, where $U_1 = |N(S_1, j\omega)|S_1$ and $\phi_U(\omega)) = \angle N(S_1, j\omega)$. The DF of the nonlinear element is defined as follows

$$N(S_1, j\omega) = \frac{U_1 \angle \phi_N(\omega)}{S_1} \tag{3}$$

After this quasi-linearization, the oscillation condition becomes the same as the Nyquist condition for marginal stability in linear feedback systems, i.e.,

$$N(S_1, j\omega)L(j\omega) + 1 = 0 \Rightarrow L(j\omega) = -\frac{1}{N(S_1, j\omega)} \tag{4}$$

Note that the accuracy of the DF approach can be improved if high order terms are included in the analysis. However, the traditional use of this approach is based only on the first harmonic component.

The intersection points of $-1/N(S_1, j\omega)$ and $L(j\omega)$ gives the possible limit cycles of the system. Depending on the behavior the linear part $L(j\omega)$ and the nonlinear part $-1/N(S_1, j\omega)$, more than one limit cycle may coexist for the same set of parameter values.

B. Describing function of the hysteresis element

The DF of the hysteresis element can be obtained by developing its output as a Fourier series. The periodic square wave u_F can be expressed by a Fourier series, as a sum of sinusoidal components at the switching frequency ω_0 and its harmonics

$$u_F(t) = \delta V_{dc} + \frac{2V_{dc}}{\pi} \sum_{n=1}^{\infty} \frac{1}{n} \sin(n\delta\pi) \cos(n\omega_0 t) \tag{5}$$

Taking the first harmonic of this series and performing the ratio between it and the amplitude of the input, the following expression for the describing function of the hysteretic controller is obtained [18]

$$N(S_1, j\omega) = \frac{U_1 \angle \phi_U}{S_1} = \frac{2V_{dc}}{\pi S_1} \left(\sqrt{1 - \frac{h^2}{S_1^2}} - j \frac{h}{S_1} \right) \tag{6}$$

[1]The terms switching frequency and oscillation frequency have been used in the paper interchangeably.

C. Study of the hysteresis controlled system without compensating network

In the complex plane, (6) is given by a real part and an imaginary term set by the relay amplitude and hysteresis width. The term $-1/N(S_1, j\omega)$, which is used for determining the possible limit cycles, is given by

$$-\frac{1}{N(S_1, j\omega)} = -\frac{\pi}{2V_{dc}}\left(\sqrt{S_1^2 - h^2} + jh\right) \qquad (7)$$

Fig. 2(a) shows the plot of this term together with the Nyquist plot of the LCL filter for the set of parameter values shown in Table I. Note that the term (7) is very small for the set of parameter values used ($1/N(S_1, j\omega) \approx 0.0017$).

According to this figure, a stable limit cycle appears in Zone A. The amplitude of the battery current corresponding to this limit cycle is $\approx \pm 50$ A and its frequency is $f_0 \approx 2.3$ kHz. These data were obtained from direct numerical simulations of the system.

Despite obtaining a stable limit cycle, its amplitude is quite high, and therefore this limit cycle is not suitable for battery charging. Moreover, the oscillation amplitude and frequency cannot be controlled by the hysteresis width.

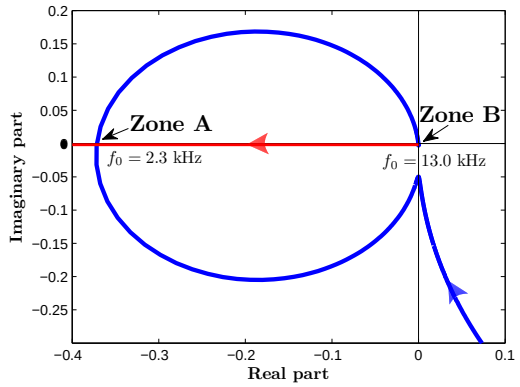

(a)

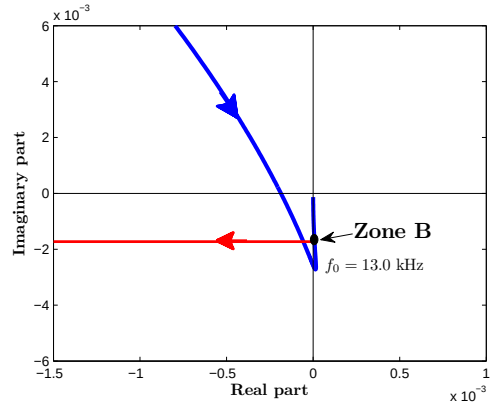

(b)

Fig. 2. Frequency response $G_c(j\omega)$ and the DF of the hysteretic relay. (a) Overall view. (b) zoom in the desired limit cycle zone.

TABLE I
PARAMETER VALUES USED UNLESS OTHERWISE NOTED. VALUES NOT STATED HERE ARE EITHER STATED IN THE TEXT OR IN THE FIGURE CAPTIONS.

Parameter	Value	Parameter	Value
	Power circuit		
r_1	0.63 Ω	L_1	4.7 mH
r_2	0.3 Ω	L_2	0.54 mH
V_{dc}	300 V	V_{bat}	124 V
C_1	10 μF		
	Control circuit		
R_f	10 kΩ	C_f	470 nF
κ_c	0.66	r_c	0.63 Ω
i^*_{bat}	±3 A	h	0.33

D. Introduction of compensating network

A necessary condition for controlled oscillations in a relay feedback system is that the relative degree of the transfer function of its linear part should not exceed 2 and that all the roots (poles and zeros) must be located in the left half side of the s-plane [19]. In the present case, as the relative degree of transfer function $L(s)$ is 3, the oscillation of the control signal σ will not be bounded between the hysteresis width limits. To overcome this problem and in order to obtain a limit cycle with different features, a compensating network is added in the feedback loop. To compensate the system, we propose to reduce the relative degree of its linear part by means of a parallel stage (dashed line in Fig. 1) with a second order transfer function $K(s)$ given by

$$K(s) = \frac{\kappa_c}{L_c s + r_c}\frac{\tau_f s}{\tau_f s + 1} \qquad (8)$$

where it can be observed that it consists of a low-pass filter (L_c, r_c) cascaded with a high-pass filter, whose time constant is $\tau_f = R_f C_f$, in a clear-cut contrast with [10] where a simple PI compensator was used.

The whole effect of these two cascaded filters is an indirect measurement of the AC component of the current i_1. As a result, after inserting the compensating network, the modified LCL filter is a system with relative degree 1 and whose transfer function $G_c(s) = I_{bat}(s)/U_F(s)$ becomes

$$G_c(s)|_{V_{bat}=0} = \frac{B_4 s^4 + B_3 s^3 + B_2 s^2 + B_1 s + B_0}{A_5 s^5 + A_4 s^4 + A_3 s^3 + A_2 s^2 + A_1 s + A_0} \qquad (9)$$

where A_k and B_k are coefficients that depend on both power plant and compensator parameters.

For $\kappa_c = 1$ and taking L_c and r_c larger than the values of L_1 and r_1 respectively, it can be ensured that all poles and zeros of the transfer function $G_c(s)$ are in the left side of the s-plane. Thus, in this range, $G_c(s)$ is a stable minimum phase system. This condition guarantees the local stability of the system. The study of the DF in the compensated system, with the parameter values considered, shows that the current in the output of $G_c(s)$ has a frequency of 3.2 kHz with an oscillation amplitude of about ≈ 50 A (Fig. 2, zone A), corresponding to a stable limit cycle but inappropriate to the battery charging as in the uncompensated system. On the other hand, in Zone B, with the same set of parameter values of Table I and for $L_c = L_1$, there exists an operating point that determines a

current output stage that provides very low ripple (less than 40 mA) and a frequency $f_0 \approx 13$ kHz, (Fig. 2, enlarged Zone B). Note that in this kind of applications, this value of switching frequency is acceptable. A relatively small ratio between L_1 and L_c makes a small amplitude limit cycle to appear in the system. In this case, an approximated expression for the oscillation frequency can be obtained by solving Eq. (4), which in the high frequency range, and assuming $S_1 = h$, can be approximated by

$$1 - \frac{2\kappa_c V_{dc}}{L_c h \pi \omega} = 0 \tag{10}$$

and when solved for ω, the following expression for the oscillation frequency f_0 is obtained

$$f_0 = \frac{\kappa_c V_{dc}}{h L_c \pi^2} \tag{11}$$

For the set of parameter values shown in Table I, a switching frequency $f_0 \approx 13$ kHz is obtained, which is in good agreement with the numerical result obtained by the graphical approach shown in Fig. 2. It is worth noting here that in spite of the good matching between these results, the DF method is an approximating approach which has some limitations. In fact, this method does not consider that the stage has asymmetrical hysteresis output levels and, is unable to determine the duty cycle under which the converter is operating. Moreover, the value of the obtained switching frequency is not accurate as it will be shown later by using either a more precise numerical frequency domain approach (Tsypkin method) [19] or a time domain analytical sliding mode approach [20].

IV. Tsypkin-based approach

The self-oscillating DC-DC bidirectional converter can be considered as a linear system with a square wave periodic input u_F. The output of the system i_{bat} will be also periodic with the same period and it will be composed of a DC component i_{bat0} and an AC component $\tilde{i}_{bat}$. According to (5) and (9), the battery current is determined by the following equation [10]

$$i_{bat}(t) = \left(\frac{V_{dc}}{2} - V_{bat}\right)|G_c(0)| + \left(\frac{V_{dc}}{2}(2\delta - 1)\right)|G_c(0)| + \frac{2V_{dc}}{\pi}\sum_{n=1}^{\infty}\frac{|G_c(n\omega_0)|}{n}\sin(n\delta\pi)\cos(n(\omega_0 t - \delta\pi) + \phi) \tag{12}$$

where δ is the duty cycle, $\phi = \angle G_c(n\omega_0)$ and $|G_c(0)|$ is the DC gain of the system. The variation of the battery current reference signal i^*_{bat} is comparatively slow with respect to the periodic term of the battery current, so that the input reference may be considered constant during the period $T = 2\pi/\omega_0$. From [19], the conditions for the existence of oscillations in this DC-DC converter are given by

$$\begin{aligned} \tilde{\sigma}(\delta T) &= \kappa(i^*_{bat} - \left(\frac{V_{dc}}{2} - V_{bat}\right)|G_c(0)| - \tilde{i}_{bat}(\delta T)) = -h \\ \tilde{\sigma}(T) &= \kappa(i^*_{bat} - \left(\frac{V_{dc}}{2} - V_{bat}\right)|G_c(0)| - \tilde{i}_{bat}(T)) = +h \\ \dot{\tilde{\sigma}}(\delta T^-) &< 0, \;\; \dot{\tilde{\sigma}}(T^-) > 0 \end{aligned} \tag{13}$$

The value of ω_0 and δ can be obtained by a frequency domain method consisting in plotting the Tsypkin locus defined by

$$\begin{aligned} T_1(\omega) &= -\frac{1}{\omega}\dot{\tilde{\sigma}}(T^-) - j\tilde{\sigma}(T) \\ T_\delta(\omega) &= -\frac{1}{\omega}\dot{\tilde{\sigma}}(\delta T^-) - j\tilde{\sigma}(\delta T) \end{aligned} \tag{14}$$

Fig. 3 depicts these curves for different values of the duty cycle δ and switching frequency. For high values of ω, the corresponding curve tends to a value in the imaginary axis delimited by the term $(2\delta - 1)|G_c(0)|$.

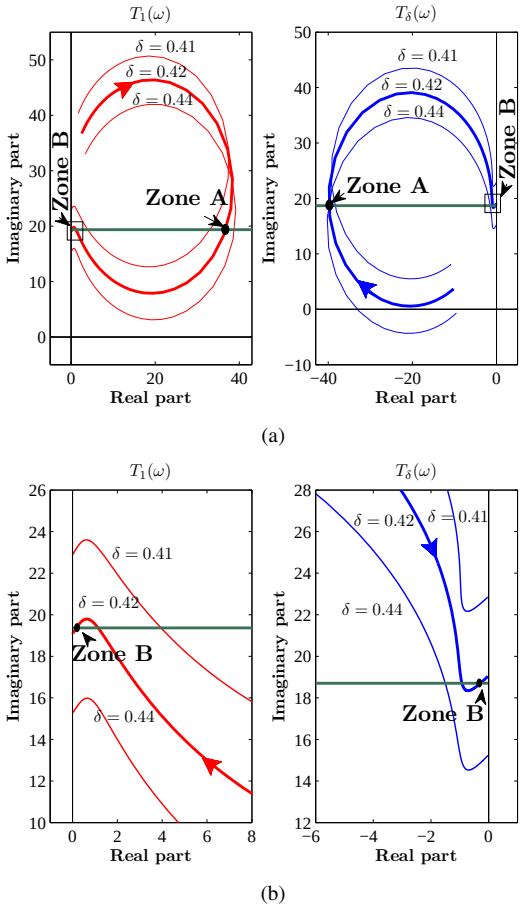

Fig. 3. Tsypkin locus for various values of duty cycles δ. (a) Overall view. (b) zoom in the desired limit cycle zone.

The Tsypkin function is a series with an infinite number of terms. However the convergence of this series is guaranteed by the fact that the transfer function $G_c(s)$ is fifth order minimum phase system with relative degree one. As a result, only the sum of the first terms of the expressions is enough to calculate the Tsypkin locus. In our case a number of terms equal to 10 was used. This is justified by the fact that $G_c(s)$ has a low pass filter behavior which allows neglecting harmonic components of order higher than 10. A limit cycle exist if the Tsypkin locus intersects the respective straight lines r_1 and r_δ given

by

$$\Re[r_1] > 0, \quad \Im[r_1] = -i^*_{bat} + h + \left(\frac{V_{dc}}{2} - V_{bat}\right)|G_c(0)|$$
$$\Re[r_\delta] < 0, \quad \Im[r_\delta] = -i^*_{bat} - h + \left(\frac{V_{dc}}{2} - V_{bat}\right)|G_c(0)| \quad (15)$$

In this case, for the same set of parameters considered above with $i^*_{bat} = +3$ A, the intersection points between the respective Tsypkin locus and straight lines r_1 and r_δ yields two possible zones A and B (Fig. 3). Zone B determines a stable limit cycle with $f_0 \approx 16.8$ kHz and $\delta = 0.42$. Zone A gives a stable limit cycle with high amplitude oscillations ($\approx \pm 50$ A) and a switching frequency f_o = 2.3 kHz. For the case of the boost mode ($i^*_{bat} = -3$), the obtained switching frequency and duty cycles are $f_0 \approx 15.2$ kHz and $\delta \approx 0.36$.

It should be noted that in addition to these stable limit cycles, another unstable one coexists with them. The oscillation switching frequency of this unstable limit cycle is $f_0 \approx 3.6$ kHz. Note also that in terms of the switching frequency and oscillation amplitude, similar results are obtained from both the DF method and the Tsypkin approach in the case of the unpractical low frequency limit cycle. However, in the case of the desirable limit cycle, the results are quite different and more accuracy is obtained from the Tsypkin method.

V. Sliding Mode Approach

A. Variable structure system model

In the above sections, the analysis of the proposed hysteretic controlled system has been performed in the frequency domain and by a numerical procedure. However, this system also allows an analysis in the time domain using an analytical approach [21], [22]. The bidirectional DC-DC converter with the compensating stage can be considered as a variable structure system which could be modeled by the following expression

$$\dot{\mathbf{x}} = (\mathbf{A}\mathbf{x} + \mathbf{d}) + (\mathbf{B}\mathbf{x} + \mathbf{c})u \quad (16)$$

where the vector of state variables is $\mathbf{x} = (i_1, v_1, i_2, i_c, v_f)'$ and matrices, $\mathbf{A}$, $\mathbf{B}$, $\mathbf{c}$ and $\mathbf{d}$ are defined by

$$\mathbf{A} = \begin{pmatrix} -\frac{r_1}{L_1} & -\frac{1}{L_1} & 0 & 0 & 0 \\ \frac{1}{C_1} & 0 & -\frac{1}{C_1} & 0 & 0 \\ 0 & \frac{1}{L_2} & -\frac{r_2}{L_2} & 0 & 0 \\ 0 & 0 & 0 & -\frac{r_c}{L_c} & 0 \\ 0 & 0 & 0 & \frac{1}{C_f} & -\frac{1}{R_f C_f} \end{pmatrix},$$
$$\mathbf{d} = \begin{pmatrix} 0 \\ 0 \\ -\frac{V_{bat}}{L_2} \\ -\frac{\kappa_c V_{bat}}{L_c} \\ 0 \end{pmatrix}, \quad \mathbf{B} = \mathbf{0}, \quad \mathbf{c} = \begin{pmatrix} \frac{V_{dc}}{L_1} \\ 0 \\ 0 \\ \frac{\kappa_c V_{dc}}{L_c} \\ 0 \end{pmatrix} \quad (17)$$

and u is the binary driving signal which is equal to 1 during the ON phase (T_1 is ON) and it is equal to 0 during the OFF phase (T_1 is OFF).

B. Equivalent control

At this point, we proceed to perform the time domain analysis of the system using the sliding mode approach based on the equivalent control method [20]. For this purpose we define the sliding surface as $\Sigma = \{\mathbf{x}|\sigma(\mathbf{x}) = 0\}$, where $\sigma(\mathbf{x})$ is given by

$$\sigma = \kappa i^*_{bat} - r\mathbf{x} = 0 \quad (18)$$

i^*_{bat} is the desired constant value of the steady state battery current and r is the feedback vector given by $r = \kappa(0, 0, 1, 1, \frac{-1}{R_f})$. The corresponding gradient of the surface is $\nabla\sigma = -r$, where ∇ stands for the gradient operator. To fulfill the transversality condition, it must be verified that the scalar product $\nabla\sigma \cdot (\mathbf{B}\mathbf{x} + \mathbf{c}) \neq 0$. This scalar product in our system is

$$\nabla\sigma \cdot (\mathbf{B}\mathbf{x} + \mathbf{c}) = -\kappa\kappa_c \frac{V_{dc}}{L_c} \quad (19)$$

It can be observed that, for $\kappa_c = 0$, the transversality condition is not fulfilled and therefore no sliding mode exists in this case. This explains why a limit cycle with both controllable frequency and amplitude does not exist as it was shown by using the DF approach. However for $\kappa_c \neq 0$, the transversality condition is clearly fulfilled and a sliding mode exists. In this case, an expression of the equivalent control u_{eq} can be determined as follows

$$u_{eq} = -\frac{\nabla\sigma \cdot (\mathbf{A}\mathbf{x} + \mathbf{d})}{\nabla\sigma \cdot (\mathbf{B}\mathbf{x} + \mathbf{c})} \quad (20)$$

This equivalent control is bounded by the minimum and maximum values of the control signal u.

$$0 < u_{eq} < 1 \quad (21)$$

In our system the expression of u_{eq} is given by

$$u_{eq} = \frac{L_c(r_2 i_2 + V_{bat} - v_1)}{L_2 \kappa_c V_{dc}} + \frac{r_c i_c + \kappa_c V_{bat}}{\kappa_c V_{dc}} + \frac{L_c(R_f i_c - v_f)}{R_f^2 C_f \kappa_c V_{dc}} \quad (22)$$

By substituting (22) in (21) we can determine the region of the design parameter space and the state space where sliding dynamics may exist. Note that the equivalent control is both state and parameter dependent.

C. Ideal sliding dynamics and its equilibrium point

The region of state space where (21) is fulfilled gives the sliding manifold where sliding dynamics exist. In this region the equations governing the dynamics of the system can be obtained by substituting in (16) the switched control signal u by the continuous equivalent control signal u_{eq}. Note that there is also an order reduction in the system dynamics due to Eq. (18). The single equilibrium point $X_{eq} = (I_{L1}, \quad I_{L2}, \quad I_c, \quad V_f)'$ of the sliding dynamics is given by

$$I_{L1} = I_2 = i^*_{bat}, \quad I_c = \frac{\kappa_c i^*_{bat}(r_1 + r_2)}{r_c}$$
$$V_1 = r_2 i^*_{bat} + V_{bat}, \quad V_f = \frac{\kappa_c i^*_{bat}(r_1 + r_2) R_f}{r_c} \quad (23)$$

The corresponding equivalent control U_{eq} for this equilibrium point is:

$$U_{eq} = \frac{(r_1 + r_2)i^*_{bat} + V_{bat}}{V_{dc}} \tag{24}$$

which corresponds to the duty cycle of the converter. Since the ideal sliding mode dynamics for the bidirectional converter is linear, the stability of the equilibrium point can be studied by applying the Routh-Hurwitz criterion to the characteristic polynomial. This polynomial is fourth order due to the order reduction imposed by the constraint defined in Eq. (18).

All constraints imposed by the Routh-Hurwitz criterion are fulfilled and therefore the equilibrium point is stable. It is worth to note that the order reduction make the stability analysis more simple due to a reduced order characteristic polynomial of the linearized system.

D. Operating switching frequency

Once the system is working in SM, it can be considered that the waveforms of the control signal σ are triangular. The switching frequency f_0 is given by:

$$f_0 = \frac{1}{T} = \frac{1}{t_{on} + t_{off}} = \frac{1}{2h}\frac{m_{on}m_{off}}{m_{on} + m_{off}} \tag{25}$$

m_{on} and m_{off} being the slopes of the control signal σ during for $u = 1$ and for $u = 0$. These slopes are given by:

$$m_{on} = \nabla\sigma \cdot \dot{\mathbf{x}}|_{u=1} = \nabla\sigma \cdot [(\mathbf{Ax} + \mathbf{d}) + (\mathbf{Bx} + \mathbf{c})] \tag{26}$$

$$m_{off} = -\nabla\sigma \cdot \dot{\mathbf{x}}|_{u=0} = -\nabla\sigma \cdot [\mathbf{Ax} + \mathbf{d}] \tag{27}$$

By substituting (26)-(27) in (25), and assuming steady state operation, the following expression for the switching frequency is obtained:

$$f_0 = \frac{\kappa\kappa_c}{2hL_cV_{dc}}((r_1+r_2)i^*_{bat}+V_{bat})(V_{dc}-V_{bat}-(r_1+r_2)i^*_{bat}) \tag{28}$$

It can be observed that this switching frequency is parameter and state dependent and that a linear relationship exists between it and the feedback compensator gain κ_c (or equivalently κ). Note that, in a hysteretic controller, the switching frequency depends on the gain κ_c and the hysteresis width h. For the system parameters considered in this paper, switching frequencies $f_0 \approx 13$ kHz and $f_0 \approx 15$ kHz are predicted from the DF and the sliding mode approaches respectively.

VI. Time domain numerical simulations

A. System performances

In order to verify the previous theoretical predictions, time domain simulations have been carried out using the switching model of the system. These simulations show that the SM dynamics is achieved in both buck and boost modes where power flows from the high voltage side V_{dc} to the low voltage side V_{bat} and vice-versa. The change from one mode to another has been carried out by inverting the sign of the reference current i^*_{bat}. Figure 4 shows the waveforms of the battery current i_{bat}, the input current i_1, the reference current i_{ref} and the switching function σ for the buck mode, the boost mode and during transition between them. The current reference is changed from -3 A to +3 A at $t = 333$ ms and from +3 A to -3 A at $t = 777$ ms. The current reference is changed gradually using a RC filter whose time constant is 1 ms. It can be observed that sliding dynamics is guaranteed before, after and ever during transition. An oscillation frequency of about 15 kHz is obtained in the buck mode which is in perfect agreement with expression (28). In the boost mode, a smaller switching frequency is obtained which can also be predicted by (28) if the sign of i^*_{bat} is inverted. It can be noted that the results given by the Tsypkin method and the SM approach are in a good matching while the DF-approach contains significant error. The accuracy of the DF approach can be improved by increasing the number of high order harmonic components but this will be at the expense of simplicity. Note also that traditional use of the DF approach, only the fundamental component is considered.

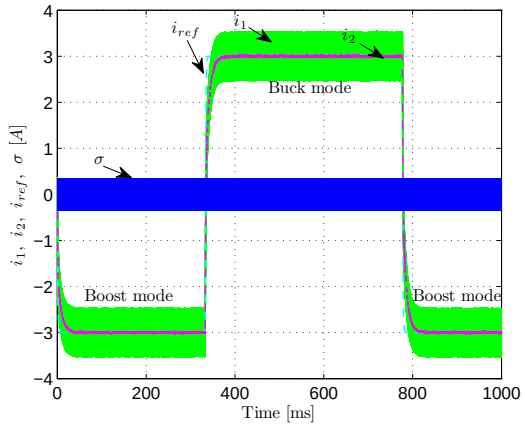

Fig. 4. Waveforms of battery current i_{bat}, input current i_1, reference current i_{ref} and switching function σ for buck mode, boost mode and during transition.

VII. Experimental Results

A. System description

To verify the theoretical hypothesis, an experimental prototype has been developed. The schematic circuit diagram of both power stage and control circuit is illustrated in Fig. 5. The implemented circuit uses a SEMIKRON educational module including: 3-phase inverter, a 1100 μF input capacitor connected at the module DC-link, and a SKHI22A up-down drivers to couple the inverter IGBT's to an external control. One of the inverter legs is the power stage of our system. It is worth noting that the maximum switching frequency limit of this module is about 18 kHz. Also, we can observe the LCL filter (L_1=4.7 mH, L_2=540 μH, C_1=10 μF) and a battery bank consisting of nine car batteries of 12 V 50 Ah connected in series.

The control stage includes two different parts. The first part is a hysteretic comparator giving the IGBT's switching signal u comparing an error signal σ with zero. The second part gives the difference σ between a current reference i^*_{bat}, and the indirect measure of i_1. This indirect measure avoids the use of an expensive hall-effect sensor and is realized combining two

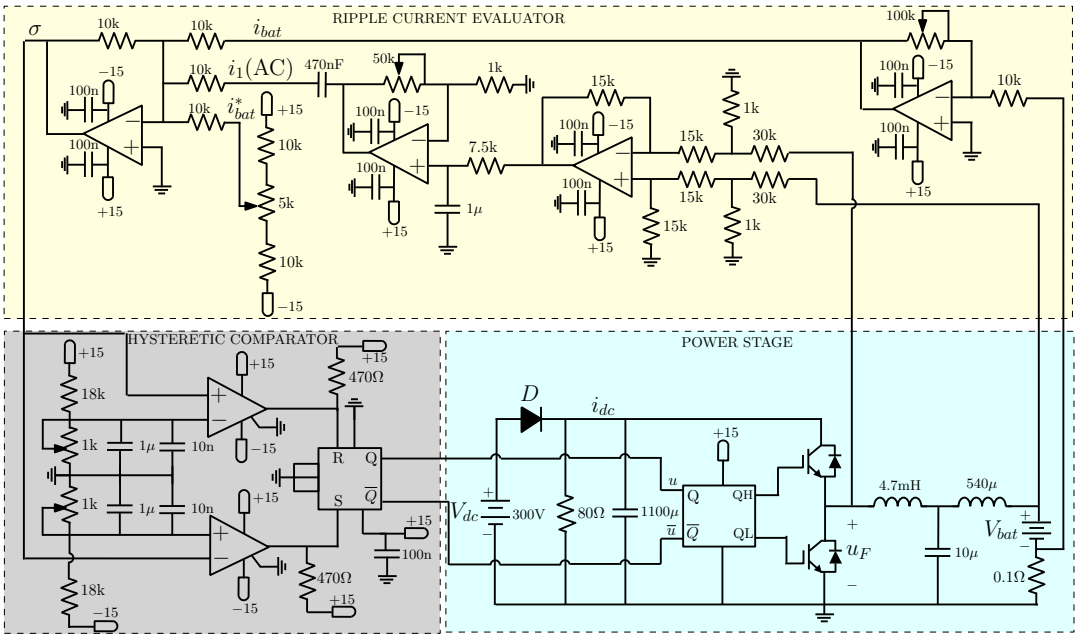

Fig. 5. Schematic circuit diagram of the experimental prototype.

signals, the battery current (average value of i_1), and the signal given by a circuit that evaluates the inductor ripple current from the voltage difference between inverter output V_f and battery voltage V_{bat}.

The system is fed by a 300 V power supply. During the discharge or boost mode, to avoid a negative current in the power supply, a series connection of a diode and a shunt resistor of about 80 Ω to dissipate the power delivered by the converter have been included. Depending on the state-of-charge, the battery bank voltage will be between 113 V and 139 V.

B. Circuit Performance

Oscilloscope captions of figure 6 show a good agreement between theoretical predictions and experimental results. The first oscilloscope caption shows a buck-mode experiment, whereas the other caption depicts a step-up (boost) mode test. In these captions, CH1 shows the current delivered by the power supply to the DC-link. CH2 shows the voltage at the half-bridge output port, where the LCL filter is connected. This signal is used to measure the system switching frequency. Channels CH3 and CH4 depict respectively the battery input current and voltage. Note that the battery current is always flat. As it can be seen in Fig. 6(a), during the buck or charging mode the current is positive, the battery voltage increases up to 139 V and the switching frequency is 16.55 kHz, whereas in the boost or discharging mode (Fig. 6(b)), the battery current is negative, the voltage decreases until 113 V, and the switching frequency is 14.93 kHz. The expected pulsating half-bridge input current i_{dc} appears smoothed by the SEMIKRON Module DC-Link 1100 μF capacitor as proven by both oscilloscope captions. Figure 7 shows the experimental measurements corresponding to the waveforms of battery current i_2, input current i_1, reference current i_{ref} and switching function σ for the different modes (buck and boost) and during transition between them. It can be observed from the detail of the control signal σ (Fig.7(b)) that sliding dynamics is maintained before, after and ever during transition as it was predicted by numerical simulations shown in Fig. 4. It is worth noting that the system keep its self-oscillating features even when the battery current is zero.

VIII. Conclusions

The dynamical behavior of a bidirectional self-oscillating DC-DC converter with a BESS has been studied in this work. Different approaches are combined in order to uncover the dynamic properties of the system. Frequency domain approaches based on DF and Tsypkin method have been used to illustrate the self-oscillation features of the system under hysteretic control. First, the system without compensating network has been proved to present a limit cycle behavior with both undesirable high amplitude and low frequency oscillation. The compensating network is designed to provide a signal proportional to the AC component of the input current in the LCL filter which results in a limit cycle with appropriate features. The sliding mode approach has shown that without compensating network, sliding mode dynamics does not exist. Then, it has been demonstrated that introducing a compensating network in the feedback loop of the current controller, results in a another practical limit cycle which corresponds to a sliding equilibrium point. The sliding mode approach is straightforward and allows to obtain analytical design criteria such as closed loop poles and steady state switching frequency that can be obtained from closed-form expressions. Experimental measurements in a low power prototype have been used to validate the numerical simulations and the detailed theoretical predictions. The study reveals that the system works appropriately in both buck and boost modes.

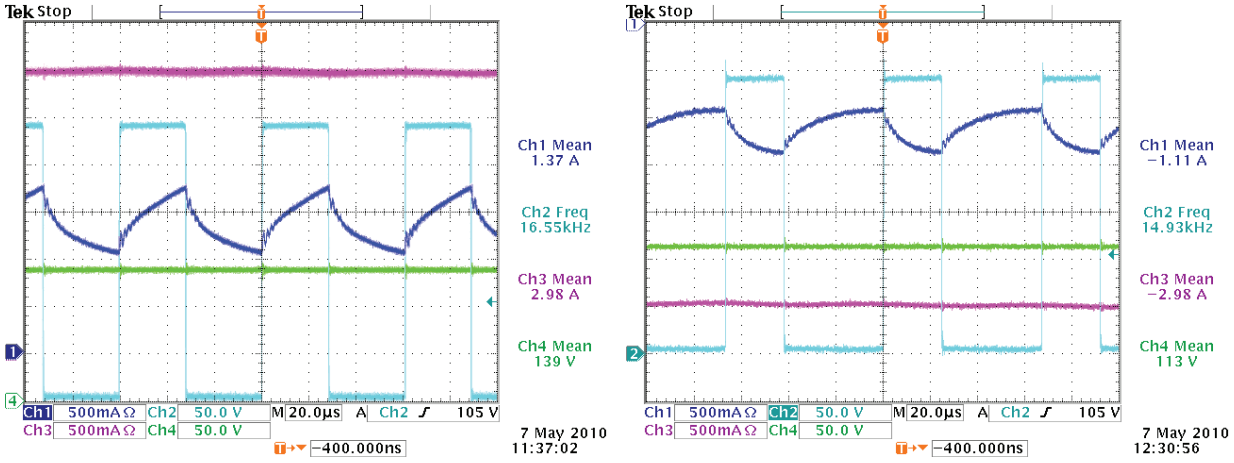

Fig. 6. Experimental time domain waveforms. (a) Current flows from V_{dc} to V_{bat} (buck mode), (b) Current flows from V_{bat} to V_{dc} (boost mode). CH1: i_{dc}, CH2: Voltage u_F, CH3: Current i_{bat}, CH4: Battery voltage V_{bat}.

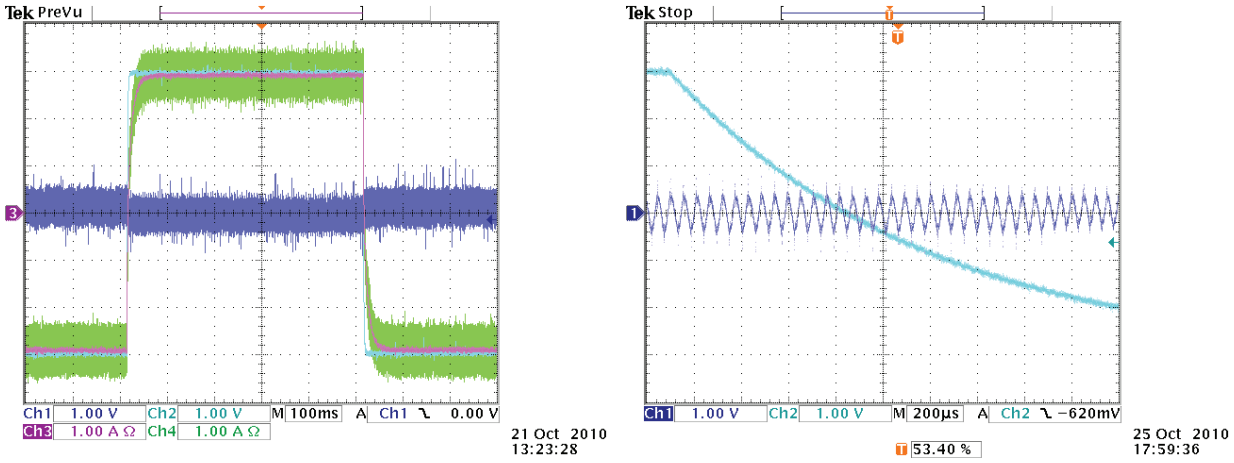

Fig. 7. Experimental time domain waveforms. (a) Response of the system when a change from the buck mode to the boost mode is required. CH1: σ, CH2: i_{ref}, CH3: i_{bat}, CH4: i_1. (b) Detail of σ and i_{ref} during transition from buck mode to boost mode showing that sliding dynamics exist and is maintained during transition. The current reference is changed gradually using a RC filter whose time constant is 1 ms.

REFERENCES

[1] S. D. Gamini Jayasinghe, D. Mahinda Vilathgamuwa, U. K. Madawala, "Direct Integration of Battery Energy Storage Systems in Distributed Power Generation," Energy Conversion, IEEE Transactions on , vol.26, no.2, pp.677-685, June 2011

[2] D. M. Sable, F. C. Lee and B. H. Cho, "A zero-voltage-switching bidirectional battery charger/discharger for the NASA EOS satellite," *IEEE Applied Power Electronics Conference and Exposition,* 1992, pp. 614-621.

[3] F. Caricchi, F. Crescimbini, F. G. Capón and L. Solero, "Study of bi-directional buck-boost converter topologies for application in electrical vehicle motor drives," *IEEE Applied Power Electronics Conference and Exposition,* 1998, pp. 287-293.

[4] L. Martinez-Salamero, J. Calvente, R. Giral, A. Poveda and E. Fossas, "Analysis of a bidirectional coupled-inductor Cuk converter operating in sliding mode," *IEEE Trans. Circuits and Systems I: Fundamental Theory and Applications,* vol. 45, pp. 355-363, Apr.

[5] R.M. Schupbach and J.C. Balda, "Comparing DC-DC converters for power management in hybrid electric Vehicles," *IEEE Electric Machines and Drives Conference,* 2003, pp. 1369-1374.

[6] J. Zhang, J-S. Lai, R-Y. Kim and W. Yu, "High-Power Density Design of a Soft-Switching High-Power Bidirectional dc-dc Converter," *IEEE Trans. Power Electronics,* vol. 22, no. 4, pp. 1145-1153, 2007.

[7] K. Jin, M. Yang, X. Ruan and M. Xu, "Three-Level Bidirectional Converter for Fuel-Cell/Battery Hybrid Power System," *IEEE Trans. Industrial Electronics,* vol. 57, pp. 1976-1986, Jun. 2010.

[8] D. Jovcic "Bidirectional, High-Power DC Transformer," *IEEE Trans. Power Delivery,* vol. 24, no. 4, pp. 2276-2283, 2009.

[9] Y. Xie, J. Sun and J. S. Freudenberg, "Power Flow Characterization of a Bidirectional Galvanically Isolated High-Power DC/DC Converter over a Wide Operating Range," *IEEE Trans. Power Electronics,* vol. 25, no. 1, pp. 54-66, 2010.

[10] J. A. Barrado; R. Griñó and H. Valderrama-Blavi; "Power-Quality Improvement of a Stand-Alone Induction Generator Using a STATCOM With Battery Energy Storage System," *IEEE Transactions on Power Delivery,* vol. 25, no. 4, pp. 2734-2741, 2010.

[11] M. Bojrup, "Advanced control of active filters in a battery charger application," Licentiate thesis, Lund University, Lund, Sweden, 1999., available at http://www.iea.lth.se/publications/Theses/LTH-IEA-1021a.pdf

[12] F. F. Judd and C-T. Chen, "On the Performance and Design of Self-Oscillating DC-to-DC Converters", *IEEE Trans. Industrial Electronics and Control Instrumentation,* vol. IECI-19, no. 3, pp. 89-97, 1972.

[13] Z. Guojo, T. Xisheng and Q. Zhiping, "Research on Battery Superca-

pacitor Hybrid Storage and Its Applications in Microgrids," *Proc. IEEE, Asia and Pacific Power and Energy Engineering Conference,* pp. 1-4, Chengdu, China, 2010.
[14] Z. Yao, L. Xiao and Y. Yan, "Dual-Buck Full-Bridge Inverter with Hysteresis Current Control," *IEEE Trans Industrial Electronics,* vol. 56, no. 8, pp. 3153-3160, 2009.
[15] A., Schild, J. Lunze, J. Krupar, W. Schwarz, "Design of Generalized Hysteresis Controllers for DC-DC Switching Power Converters," *IEEE Transactions on Power Electronics,* vol. 24, no. 1, pp. 138-146, 2009.
[16] S. C. Huerta, P. Alou, J. A. Oliver, O. Garcia, J. A. Cobos, A. M. Abou-Alfotouh, "Nonlinear Control for DC-DC Converters Based on Hysteresis of the C_{rmOUT} Current With a Frequency Loop to Operate at Constant Frequency," *IEEE Transactions on Industrial Electronics,* vol. 58, no. 3, pp. 1036-1043, 2011.
[17] T. Jen-Chieh, C. Chi-Lin. L. Yu-Huei, Y. Hong-Yuan, H. Ming-Shen, C. Ke-Horng, "Modified Hysteretic Current Control (MHCC) for Improving Transient Response of Boost Converter," *IEEE Transactions on Circuits and Systems I: Regular Papers,* vol. 58, no. 8, pp. 1967-1979, 2011.
[18] A. Gelb and W. E.Vander Velde, *Multiple-Input Describing Function and Nonlinear System Design*, New York: McGraw-Hill, 1968.
[19] Y. Z. Tsypkin, *Relay control systems,* United Kingdom: Cambridge University Press, 1984.
[20] V. Utkin, J. Guldner and J. Shi, *Sliding mode control in electro-mechanical systems, 2n Ed.*, London, CRC Press, 2009.
[21] L. Martinez-Salamero, H. Valderrama-Blavi, R. Giral, C. Alonso, B. Estibals and A. Cid-Pastor, "Self-Oscillating DC-to-DC Switching Converters with Transformer Characteristics," *IEEE Trans. Aerospace and Electronic Systems,* vol. 41, pp. 710-716, 2005.
[22] Y. Chen and Y. Kang, "The Variable-Bandwidth Hysteresis-Modulation Sliding-Mode Control for the PWM-PFM Converters," *IEEE Transactions on Power Electronics,* vol. 26, no. 10, pp. 2727-2734, 2011.

José Antonio Barrado received the electronic engineering degree from the Universitat de Barcelona (UB), Spain, in 2000 and the Ph.D. degree in automatic control from Universitat Politècnica de Catalunya (UPC), Barcelona, Spain, in 2008. He is currently an Assistant Professor with the Department of Electronic Engineering and Automatic Control of the Universitat Rovira i Virgili, Tarragona, Spain. His research interests include analysis, modeling and control of electric generators and power converters applied to renewable energy systems.

Abdelali El Aroudi (M'00) was born in Tangier (Morocco), in 1973. He obtained the graduate degree in physical science from Faculté des sciences, Université Abdelmalek Essadi, Tetouan, Morocco, in 1995, and the Ph.D degree (with honors) from Universitat Politècnica de Catalunya, Barcelona, Spain in 2000. During the period 1999-2001 he was a visiting Professor at the Department of Electronics, Electrical Engineering and Automatic Control, Technical School of Universitat Rovira i Virgili (URV), Tarragona, Spain, where he became an associate professor in 2001 and a full-time tenure Associate Professor in 2005. During the period September 2007-January 2008 he was holding a visiting scholarship at the Department of Mathematics and Statistics, National University of Colombia, Manizales, conducting research on modeling of power Electronics circuits for energy management. From February 2008 to July 2008, he was a visiting scholar at the *Centre de Recherche en Sciences et Technologies de Communications et de l'Informations* (CReSTIC), Reims, France. His research interests are in the field of structure and control of power conditioning systems for autonomous systems, power factor correction, stability problems, nonlinear phenomena, chaotic dynamics, bifurcations and control. He has published more than 100 papers in scientific journals and conference proceedings. He is a member of the GAEI research group (Rovira i Virgili University) on Industrial Electronics and Automatic Control whose main research fields are power conditioning for vehicles, satellites and renewable energy.

Hugo Valderrama-Blavi (S'94) received the ingeniero de telecomunicación degree from the Universidad Politécnica de Catalunya, Barcelona, Spain, in 1994. He is currently an Assistant Professor in the Departamento de Ingeniería Electrónica, Eléctrica y Automática, Escuela Técnica Superior de Ingeniería, Universitat Rovira i Virgili, Tarragona, Spain, where he is working in the field of inverters for photovoltaic systems.He is a member of the GAEI research group on Industrial Electronics and Automatic Control, whose main research fields are power conditioning for vehicles, satellites and renewable energy. He is also a member of the IEEE.

Javier Calvente (S'94-M'03) received his degree in Telecommunication Engineering in 1994 from the Universitat Politècnica de Catalunya (UPC), Barcelona, Spain. He was a visiting scholar at Alcatel Space Industries in Toulouse, France, in 1998. He received his Ph.D. degree from UPC in 2001. He is currently an Associate Professor at the Department of Electronics, Electrical Engineering and Automatic Control (DEEEA), Technical School of Engineering (ETSE), Rovira i Virgili University (URV), Tarragona, Spain, where he is working in the field of control of power converters. He is a member of the GAEI research group on Industrial Electronics and Automatic Control, whose main research fields are power conditioning for vehicles, satellites and renewable energy. He is also a member of the IEEE.

Luis Martínez-Salamero received the Ingeniero de Telecomunicación and the doctorate degrees from the Universidad Politécnica de Cataluña, Barcelona, Spain in 1978 and 1984, respectively. From 1978 to 1992, he taught circuit theory, analog electronics and power processing at Escuela Técnica Superior de Ingenieros de Telecomunicación de Barcelona. During the academic year 1992-93 he was visiting professor at the Center for Solid State Power Conditioning and Control, Deparment of Electrical Engineering, Duke University, Durham, NC. He is currently a full professor at the Departamento de Ingeniería Electrónica, Eléctrica y Automática, Escuela Técnica Superior de Ingeniería, Universidad Rovira i Virgili, Tarragona, Spain. During the academic years 2003-2004 and 2010-2011, he was visiting scholar at the Laboratoire d´Architecture et d´Analyse des Systèmes (LAAS) of the Research National Center (CNRS) in Toulouse, France. Dr Martínez was guest editor of the IEEE Transactions on Circuits and Systems (Vol 44, Nº8, August 1997) for the special issue on Simulation, Theory and Design of Switched-Analog Networks. He has been distinguished lecturer of the IEEE Circuits and Systems Society in the period 2001-2002. His research interests are in the field of structure and control of power conditioning systems for autonomous systems. He has published a great number of papers in scientific journals and conference proceedings and holds a US patent on the electric energy distribution in vehicles by means of a bidirectional DC-to -DC switching converter. He is the director of the GAEI, research group on Industrial Electronics and Automatic Control whose main research fields are power conditioning for vehicles, satellites and renewable energy. Dr Martínez-Salamero was the president of the IEEE Spanish Joint Chapter of the IEEE Power Electronics and the Industrial Electronics Societies in the period 2005-2008.